New Phytologist

Research

Spatiotemporal changes in gibberellin content are required for soybean nodulation

Xitong Chu[1], Huanan Su[1,2], Satomi Hayashi[1,3], Peter M. Gresshoff[1] and Brett J. Ferguson[1]

[1]Integrative Legume Research Group, School of Agriculture and Food Sciences, The University of Queensland, St Lucia, Brisbane, Qld 4072, Australia; [2]National Navel Orange Engineering Research Center, Gannan Normal University, Ganzhou, China; [3]Centre for Agriculture and Biocommodities, Queensland University of Technology, Brisbane, Qld 4000, Australia

Author for correspondence:
Brett J. Ferguson
Email: b.ferguson1@uq.edu.au

Received: *28 March 2021*
Accepted: *24 November 2021*

New Phytologist (2022) **234:** 479–493
doi: 10.1111/nph.17902

Key words: legumes, nitrogen fixation, nodulation, plant hormones, plant signalling and development, soybean, symbiosis.

Summary

- The plant hormone gibberellin (GA) is required at different stages of legume nodule development, with its spatiotemporal distribution tightly regulated. Transcriptomic and bioinformatic analyses established that several key GA biosynthesis and catabolism enzyme encoding genes are critical to soybean (*Glycine max*) nodule formation.
- We examined the expression of several GA oxidase genes and used a Förster resonance energy transfer-based GA biosensor to determine the bioactive GA content of roots inoculated with DsRed-labelled *Bradyrhizobium diazoefficiens*. We manipulated the level of GA by genetically disrupting the expression of GA oxidase genes. Moreover, exogenous treatment of soybean roots with GA_3 induced the expression of key nodulation genes and altered infection thread and nodule phenotypes.
- *GmGA20ox1a*, *GmGA3ox1a*, and *GmGA2ox1a* are upregulated in soybean roots inoculated with compatible *B. diazoefficiens*. *GmGA20ox1a* expression is predominately localized to the transient meristem of soybean nodules and coincides with the spatiotemporal distribution of bioactive GA occurring throughout nodule organogenesis. *GmGA2ox1a* exhibits a nodule vasculature-specific expression pattern, whereas *GmGA3ox1a* can be detected throughout the nodule and root. Disruptions in the level of GA resulted in aberrant rhizobia infection and reduced nodule numbers.
- Collectively, our results establish a central role for GAs in root hair infection by symbiotic rhizobia and in nodule organogenesis.

Introduction

Complex signalling networks are essential for legume–rhizobia recognition and subsequent nodule development (Ferguson *et al.*, 2010; Ferguson & Mathesius, 2014; Lin *et al.*, 2020). Gibberellin (GA) is a plant hormone and key factor required for a range of plant developmental processes, including legume nodulation. An optimum level of GA is vital for the symbiosis to be successful (S. Hayashi *et al.*, 2014). Exogenous application of GA_3 leads to altered nodulation phenotypes in pea plants, with low concentrations promoting nodulation and high concentrations inhibiting it (Ferguson *et al.*, 2005). In *Lotus japonicus*, GA_3 application can trigger spontaneous nodule formation commencing with GA-induced cell divisions of the pericycle (Kawaguchi *et al.*, 1996). In addition, treatment with various GA inhibitors, such as chlormequat chloride, paclobutrazol (PAC), and daminozide, have been shown to reduce lateral root base nodulation in *Sesbania rostrata* (Lievens *et al.*, 2005).

Biosynthesis of GA requires enzymes such as GA20 oxidase (GA20ox), which is a rate-liming factor that catalyses a series of intermediate steps in GA production (Hedden, 2020). In addition, GA3 oxidase (GA3ox) has a key role acting to catalyse the final step in the production of bioactive GA (Hedden & Kamiya, 1997; Yamaguchi, 2008). Differential expression of genes encoding these enzymes has been reported during legume nodulation (Lievens *et al.*, 2005; Hayashi *et al.*, 2012). In soybean (*Glycine max*), *GmGA20ox1a* (Glyma.04g244200) is induced in roots 12 h post inoculation (hpi) and remains upregulated in 1-wk-old nodules. In addition, *GmGA3ox1a* (Glyma.15g012100) is upregulated in multiple tissues throughout different stages of nodulation (Hayashi *et al.*, 2012). In *S. rostrata*, *SrGA20ox1* is first upregulated in cells involved in nodule primordia formation and infection, followed by those that are devoted to expanding (Lievens *et al.*, 2005). In pea (*Pisum sativum*), GA biosynthesis mutants exhibit reduced nodule numbers and aberrant nodule structures, with their phenotype rescued by exogenous application of bioactive GA (Ferguson *et al.*, 2005, 2011).

In addition to biosynthesis, the catabolism of bioactive GA is also vital to maintain GA homeostasis. To achieve this, another GA oxidase, called GA2 oxidase (GA2ox), catabolizes bioactive GA and its immediate precursors (Yamaguchi, 2008; Hedden, 2020). Recently, a *GA2ox* gene of *Medicago truncatula* has been reported to help fine-tune GA catabolism during nodule formation (Kim *et al.*, 2019). Taken together with the differential

expression patterns of GA biosynthesis genes across different legume species, these findings suggest that tight control over the GA content and its spatial–temporal availability may be essential for successful nodule organogenesis to occur.

Perception of GA occurs via a soluble receptor called gibberellin insensitive dwarf (GID; Ueguchi-Tanaka *et al.*, 2005; Murase *et al.*, 2008; Sun, 2011). Detection of the hormone facilitates the destruction of DELLA proteins, which are transcriptional repressors of GA signalling (Silverstone *et al.*, 1998; Harberd *et al.*, 2009). In *M. truncatula*, elevated GA signalling inhibits rhizobia infection in a DELLA-dependent manner (Fonouni-Farde *et al.*, 2016, 2017; Jin *et al.*, 2016). The number of infection threads (ITs) is reduced in *Mtdella* mutants, resulting in impaired nodule formation (Jin *et al.*, 2016). DELLA-mediated GA signalling impacts nodule formation through an interaction with the nodule signalling pathway 2 (NSP2)/NSP1 complex and activates nod factor-induced gene expression (Fonouni-Farde *et al.*, 2016; Jin *et al.*, 2016). Maekawa *et al.* (2009) also reported that a DELLA-NSP2-nodule inception (NIN; Schauser *et al.*, 1999) pathway was disrupted by high doses of GA_3 application. Moreover, it has been shown that GA positively regulates expression of *NIN* (Akamatsu *et al.*, 2021), which functions in the early symbiotic signalling pathway (Schauser *et al.*, 1999; Soyano *et al.*, 2013). A *nin* mutant, *daphne*, that has reduced NIN function exhibited excessive infection but no cortical cell division (Yoro *et al.*, 2014). Taken together, these results further suggest that precise GA levels in different root tissues and at different times are crucial for enabling rhizobia infection and nodule formation.

In this study, we show that bioactive GA is required for soybean nodule primordium establishment and subsequent persistence of the transient nodule meristem. Our findings also demonstrate a temporary burst in the level of bioactive GA in root cells undergoing nodule initiation. We revealed that changes in the level of bioactive GA, or the rate of GA biosynthesis and catabolism, can considerably alter nodule formation and that multiple GA oxidase genes are critical to this regulation. Changes in GA content can also influence the number of ITs and impact their ability to extend within the infected root hair. Moreover, two key nodulation genes, *NIN* and *ENOD40*, are both significantly upregulated by GA, even in the absence of rhizobia, providing additional new insight into the molecular mechanisms driving the symbiosis. Overall, GAs play a central role in regulating rhizobia infection and are essential for facilitating the development of the nodule structure.

Materials and Methods

Plant and bacterial growth conditions

The soybean (*G. max*) cv Bragg and its isogenic supernodulation mutant (*nts382*) were used in this study. Surface-sterilized seeds were germinated in 4 l black pots containing sterile grade 2 vermiculite. Emerging seedlings were then transferred into extended CYG germination pouches (triple standard length; 52.5 cm × 16 cm; Mega International, West St Paul, MN, USA) or grown in pots as per experimental requirements. Seed germination and seedling growth occurred in either a growth cabinet (16 h : 8 h, light : dark, 28°C : 26°C, 70% humidity) or a temperature-controlled glasshouse under natural light conditions (University of Queensland, Brisbane, Qld, Australia). Seedlings were watered every 3 d with sterile B&D solution (Broughton & Dilworth, 1971) supplemented with 0.5 mM potassium nitrate.

Bradyrhizobium diazoefficiens strain USDA110 and its isogenic mutant AN122 (*nodC*$^{-}$ mutant; Nieuwkoop *et al.*, 1987) were cultured in yeast mannitol broth (YMB; Vincent, 1970) at 28°C for 3 d and diluted to $OD_{600} \approx 0.1$ before inoculation.

Escherichia coli (XL1-Blue and HB101) and *Agrobacterium rhizogenes* (K599) were cultured at 37°C and 28°C, respectively, in either liquid lysogeny broth (LB) or LB agar plates containing appropriate antibiotics.

Vector constructions and soybean hairy root transformation

All sequence information of *G. max* was acquired from Phytozome v.12.1 (https://phytozome-next.jgi.doe.gov/), with sequence IDs provided in Supporting Information Table S1. All DNA fragments were amplified via PCR with proofreading DNA polymerases (Takara PrimeSTAR GXL DNA polymerase or PrimeSTAR Max DNA polymerase) using either genomic DNA or complementary DNA (cDNA) as a template. A list of primers used in this study is provided in Table S2.

Promoter:β-glucuronidase (*GUS*) constructs were generated by cloning the promoter region of *GmGA20ox1a*, *GmGA3ox1a*, and *GmGA2ox1a* (2654 bp, 2616 bp, and 1869 bp, respectively) into a modified version of the binary vector *pCAMBIA1305.1* (*pCAMBIA1305.1-Δ35Sx2*; Corcilius *et al.*, 2017). To generate overexpressing constructs, the coding sequences of *GmGA20ox1a* (1077 bp) and *GmGA2ox1a* (1071 bp) were amplified from 1-wk-old nodule cDNA using gene-specific primers (Table S2) incorporating appropriate restriction enzyme sites and cloned directly downstream of the cauliflower mosaic virus 35S promoter of either the *p15SOR* (developed in house) integrative vector or the *pORE-O4* (AY562542) binary vector (Coutu *et al.*, 2007). Two transcript variants were predicted for *GmGA20ox1a* in Phytozome v.12.1. The version used for cloning came from 1-wk-old nodule cDNA and was 60 bp shorter at the end of the second exon than the other predicted transcript variant (Fig. S1a,b). For CRISPR/Cas9 constructs, single guide RNA (sgRNA) sequences (20 bp fragments) for target genes were determined using the 'Find CRISPR Sites' feature of Geneious (v.10.0.6; Biomatters Ltd, Auckland, New Zealand; https://www.geneious.com). Target sites for CRISPR/Cas9 were scored against the *G. max* genome Wm82.a2.v1 (Phytozome v.12.1). sgRNAs targeting the same pair of duplicate genes were introduced into the binary vector *pCas9-GmU6-sgRNA* (Sun *et al.*, 2015) in a tandem manner (154 bp-spaced) by using the restriction enzymes *Eco*RI and *Hin*dIII.

Integrative vector constructs were introduced into *A. rhizogenes* strain K599 via triparental mating, whereas binary vector constructs were introduced by electroporation. *Agrobacterium rhizogenes* strains of K599 transformed with recombinant plasmids

were selected using appropriate antibiotics (listed in Table S3) and confirmed by PCR using gene-specific primers. *Agrobacterium*-mediated transgenic hairy roots were generated using methods previously developed in our laboratory (Kereszt *et al.*, 2007). Two GA biosensor binary constructs, *p16-nlsGPS1* (gibberellin perception sensor 1 (GPS1)) and the corresponding negative control *p16-nlsGPS1-NR* (Rizza *et al.*, 2017), were introduced into *A. rhizogenes* strain K599 by electroporation. LB medium plates containing 100 μg ml^{-1} spectinomycin were used for selecting the transformed bacteria.

To generate compatible soybean rhizobia containing the DsRed reporter, the *pBjGroESL4::DsRed2* construct (M. Hayashi *et al.*, 2014) was transformed into *E. coli* strain HB101 via heat shock transformation. Triparental mating (Ditta *et al.*, 1980) was subsequently performed using this modified HB101 strain, together with an HB101 strain harbouring the helper plasmid *pRK2013* and *B. diazoefficiens* strain USDA110. After mating, the bacteria were cultured on YMB selective medium containing 100 μg ml^{-1} spectinomycin and 50 μg ml^{-1} chloromycetin. The resultant colonies were restreaked and positive colonies confirmed via PCR (primer sequences available in Table S2).

Plant tissue harvests and exogenous hormone treatments

For nodulation studies, 150 ml of inoculum was applied per pot, and roots were harvested 14 d post inoculation (dpi), unless specified otherwise. Nodule number was normalized either by root FW or DW. Nodule diameter was measured using a Zeiss stereomicroscope (Stemi 2000-C) with ZEN BLUE v.2.6 (Zeiss, Jena, Germany) built-in graphics tools.

To establish the zone of nodulation (ZON) prior to inoculation, root tips and the site of the first mature root hairs were marked on plants grown in growth pouches. The time-course inoculation experiment was described previously in Hayashi *et al.* (2012).

Exogenous GA_3 and PAC were applied to roots twice per week until harvest. Concentrations of 10^{-4}, 10^{-6}, and 10^{-9} M were made by diluting 10^{-2} M stock solutions with MilliQ water, with 150 ml applied per pot or 10 ml per pouch. The treatments commenced 4 d after planting or at the same time with rhizobia inoculation.

RNA extraction, complementary DNA synthesis, and reverse transcription quantitative real-time PCR analysis

All reverse transcription (RT)-quantitative real-time PCR (qPCR) samples were harvested, snap-frozen in liquid nitrogen (N_2), and stored at −80°C until use. RNA was isolated using a Maxwell RSC Instrument with the Maxwell RSC Plant RNA Kit (Promega, Madison, WI, USA) following the manufacturer's instructions. cDNA was synthesized from 500 ng of total RNA in a 20 μl reaction using SuperScript III reverse transcriptase (Invitrogen, Waltham, MA, USA). qPCR was performed on the LightCycler 96 instrument (Roche, Basel, Switzerland) or CFX384 real-time system (Bio-Rad, Hercules, CA, USA) with the Bio-Rad CFX Maestro 1.1 using PowerUp SYBR green master mix (Applied Biosystems, Waltham, MA, USA) or GoTaq qPCR master mix (Promega). Relative expression for the genes of interest was normalized against *GmCons6* (Libault *et al.*, 2008) or *GmATPsynthase*. Gene-specific primers are listed in Table S2.

Histochemical analysis of promoter-driven β-glucuronidase expression

GUS staining was achieved by vacuum infiltrating and then incubating hairy roots in a GUS reaction solution (100 mg ml^{-1} X-Gluc; 100 mM potassium ferricyanide; 100 mM potassium ferrocyanide; 0.5 M EDTA at pH 8.0) at 37°C for 6–12 h after cell fixation in 0.5% paraformaldehyde (Jefferson *et al.*, 1987). Cross-section images were obtained by embedding 1 cm root segments in agarose blocks (4–6%) followed by sectioning on a vibratome VT1200S (Leica, Wetzlar, Germany). Bright-field pictures were captured by Nikon (Tokyo, Japan) CCD cameras (Nikon DS-Fi2 or Nikon DS-Ri1) linked with a stereomicroscope (Nikon C-PS) or a standard optical microscope (Nikon Eclipse E600).

Fluorescence microscopy

nts382 plants were inoculated with *DsRed*-expressing *B. diazoefficiens* and treated with either 10^{-6} M GA_3 or distilled water (control). Roots were harvested 7 dpi for analysis of ITs and nodule morphology. ZON segments 1 cm in length were embedded in 4% agarose blocks and hand sectioned. For root imaging, a Zeiss 700 M confocal microscope with Zeiss EC Plan-Neofluar 10×/0.30 M27 and LD LCI 25×/0.8 Imm Korr (ultraviolet) visible–infrared objectives was used. The DsRed protein was excited by a 555 nm laser, and emitted fluorescence was collected from the 525–640 nm wavelength range. The laser power exciting the sample was 2% with detector gain set to 720 and transmitted light detector gain set to 240 for imaging. The length of the IT was measured using the ZEN BLACK v.2.3 (Zeiss) built-in graphics tools.

To investigate endogenous GA gradients during nodulation, hairy roots expressing either *p16-nlsGPS1* or *p16-nlsGPS1-NR* (control) were inoculated with *B. diazoefficiens* strain USDA110 expressing DsRed and harvested at 14 dpi. *p16-nlsGPS1*-transformed roots were identified based on the presence of cyan fluorescent protein (CFP) and yellow fluorescent protein (YFP) in the root cell nucleus. To excite CFP (the donor fluorophore) and YFP (the acceptor fluorophore), 405 nm and 488 nm lasers were employed, respectively. Both laser lines were set to 5%. For fluorescence emission, 460–490 nm and 525–560 nm were set for CFP and YFP detection, respectively, with detector gain set to 750 for imaging. Additionally, an energy transfer fluorescence reading from donor to acceptor (excitation 448 nm; emission 525–560 nm) was measured. The *z*-stacks were acquired using a step-size of 1.5–2 μm, depending on the sample. A ratio of DxAm (donor excitation acceptor emission) : DxDm (donor excitation donor emission) was calculated as an approximation of a Förster resonance energy transfer (FRET) ratio. Image processing and analysis were performed using IMAGEJ (Rizza *et al.*, 2019).

Bioinformatics analysis

Amino acid sequences of GA oxidases were obtained from PHYTOZOME v.12.1 and aligned using the online program CLUSTAL OMEGA (https://www.ebi.ac.uk/Tools/msa/clustalo/). GA oxidase proteins are characterized by two functional domains: DIOX_N (PF14226) and 2OG-FeII_Oxy (PF03171). Functional GA oxidase sequences of *Arabidopsis thaliana* were used as queries to BLAST against the whole genome sequences of soybean (Schmutz *et al.*, 2010), *Phaseolus vulgaris* (common bean; Schmutz *et al.*, 2014), *M. truncatula* (Tang *et al.*, 2014), *Solanum lycopersicum* (Tomato Genome Consortium, 2012), and *Parasponia andersonii* (van Velzen *et al.*, 2018) in PHYTOZOME and *Lotus japonicus* in LOTUS BASE (Sato *et al.*, 2008; Mun *et al.*, 2016; https://lotus.au.dk/). Phylogenetic trees were constructed using MEGA-X and were derived using the maximum likelihood approach (1000 bootstraps).

Evaluation of CRISPR/Cas9-mediated gene editing

Individual hairy roots were isolated and stored separately. To minimize the impact on root DW, only *c.* 1 cm of the root tip was used for DNA isolation. PCR reactions were performed using the dilution protocol of Phire plant Direct PCR Kit (ThermoFisher Scientific, Waltham, MA, USA), according to the manufacturer's instruction. Hairy roots were screened using PCR amplification of a fragment of the *pCas9-GmU6-sgRNA* vector, with the PCR products being run on a 1% agarose gel. The presence of the target band indicated that the corresponding hairy roots were successfully transformed.

To identify the predominant types of insertions and deletions (indels) in the targeted sequences (i.e. gene edits), the regions flanking the targeted sites were amplified by PCR from both empty vector (EV) and *GmGA20ox1*, *GmGA3ox1*, and *GmGA2ox1* CRISPR/Cas9 binary vector transformed hairy roots. PCR products from these experiments (1000–1500 bp in length) were sent to the Australian Genome Research Facility (Brisbane, Australia) for Sanger sequencing. Evaluation of gene editing using sequence chromographs was validated using TIDE (Brinkman *et al.*, 2014; https://tide.nki.nl) and ICE v.2 CRISPR analysis tool (https://ice.synthego.com). All primers used in this assay are listed in Table S2.

Statistical analyses

Statistical analyses were performed using GraphPad PRISM 9.1.2 (GraphPad Software, San Diego, CA, USA). Data were analyzed using Student's *t*-test or one-way ANOVA. Statistically significant differences are labelled with asterisks (*, $P<0.05$; **, $P<0.01$; ***, $P<0.001$; ****, $P<0.0001$; ns, not significant).

Results

Rhizobia inoculation induces a transient burst in the expression of GA biosynthesis and catabolism genes

RNA sequencing (RNA-seq) was used to assess the expression of nodulation-associated genes in the ZON of soybean roots harvested 48 h after inoculation with either wild-type (WT) or an incompatible mutant (*nodC*$^-$) strain of *B. diazoefficiens* (Hayashi *et al.*, 2012). This was followed by a time-course expression study using RT-qPCR. The GA biosynthesis genes *GmGA20ox1a* and *GmGA3ox1a* were found to be upregulated in expression when inoculated with WT rhizobia, peaking at 12 hpi (Fig. 1a,b). Interestingly, a GA catabolism gene, *GmGA2ox1a* (Glyma.02g010100), was also induced, peaking slightly later at 24 hpi (Fig. 1c). This lag in expression between the genes could indicate a burst in GA production followed by the breakdown of the hormone. Expression of all three GA oxidase genes remained low to nearly undetectable in *nodC*$^-$ rhizobia-inoculated samples. Collectively, these results indicate a temporal spike in the endogenous GA content during early nodule initiation.

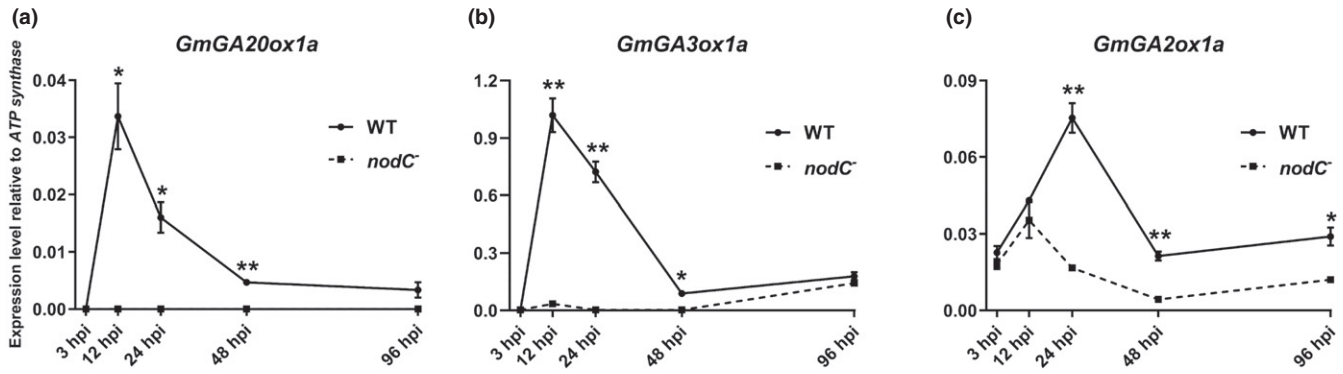

Fig. 1 Expression of GA oxidase genes during early stages of soybean nodulation. Transcript abundance of (a) *GmGA20ox1a*, (b) *GmGA3ox1a*, and (c) *GmGA2ox1a* was analyzed by reverse transcription-quantitative real-time PCR using RNA isolated from wild-type (WT) or incompetent (*nodC*$^-$) *Bradyrhizobium diazoefficiens-inoculated* soybean root tissues at 3, 12, 24, 48, and 96 h post inoculation (hpi). Error bars indicate the SEMs resulting from three biological replicates. Roots from six to eight plants were used for each experiment. Asterisks represent statistically significant differences between inoculation treatments at the same time-point (Student's *t*-test; *, $P<0.05$; **, $P<0.01$). Panels (a) and (b) are reproduced from Hayashi *et al*. (2012), with kind permission from *Plant Biotechnology Journal*.

Expression of *GmGA20ox1a* and *GmGA2ox1a* is nodulation specific

Promoter:GUS fusions were used to analyse the expression of GA oxidase genes in transgenic soybean hairy roots. *GmGA20ox1a* promoter-driven *GUS* expression was detected in the outer cortex and pericycle of the root 3 dpi with WT *B. diazoefficiens* (Fig. 2a I). This is the region of the root where the earliest cell divisions in soybean nodulation occur. By 5–7 dpi, *GUS* expression was predominantly localized to the nodule primordia (Fig. 2a II,III), and by 10–12 dpi it was concentrated in the central region of young developing nodules (Fig. 2a IV–VI). Cross-sections of these nodules established that the expression was localized to dividing/expanding cortical cells (Fig. 2b I–III) but not the invasion zone. From 14 dpi onwards, *GmGA20ox1a* promoter activity was greatly reduced, becoming undetectable in well-established nodules (Fig. 2b IV).

Similar to that observed for *GmGA20ox1a pro:GUS* transformed roots, *GmGA2ox1a* promoter activity was detected in nodules but nowhere else on the roots. This signifies that these genes are both nodule specific in their expression. *GmGA2ox1a pro:GUS* expression was not seen in early stages of nodulation but became apparent in the nodule primordia by 5 dpi (Fig. 3a I). This delayed pattern of activity between *GmGA2ox1a* and *GmGA20ox1a* promoters is consistent with the lag observed in the expression of these two genes via RT-qPCR (Fig. 1a,c). A detailed histological analysis established that *GmGA2ox1a* promoter activity was restricted to the nodule vasculature of developing nodules, becoming undetectable in mature nodule structures (Fig. 3a II–IV, b I–IV).

Unlike the nodulation-specific promoter activity of *GmGA20ox1a* and *GmGA2ox1a*, the promotor activity of *GmGA3ox1a* was detected throughout the root, irrespective of whether a compatible or incompatible strain of *B. diazoefficiens*

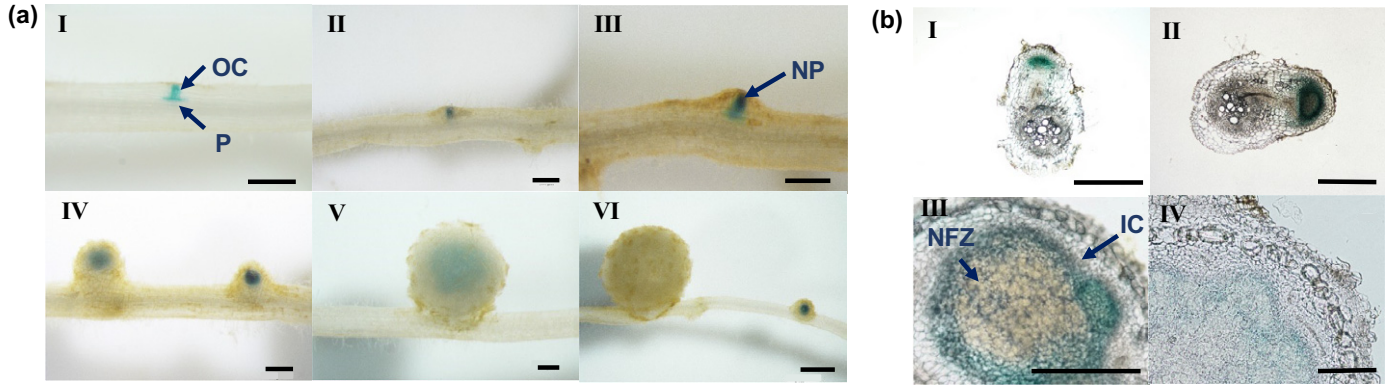

Fig. 2 Expression pattern of *GmGA20ox1a* in response to rhizobia inoculation. (a) *GmGA20ox1a* promoter activity was investigated histochemically in soybean hairy roots carrying *GmGA20ox1a pro:GUS* construct (*GUS*, *β-glucuronidase*). I–VI are root/nodule representatives at 3, 5, 7, 10, 12, and 14 d post inoculation (dpi), respectively. (b) Cross-sections of *GmGA20ox1a pro:GUS-transformed* soybean nodules at (I) 5, (II) 7, (III) 12, and (IV) 14 dpi. Bar, 500 μm. OC, outer cortex; P, pericycle; NP, nodule primordia; IC, inner cortex; NFZ, nitrogen-fixing zone.

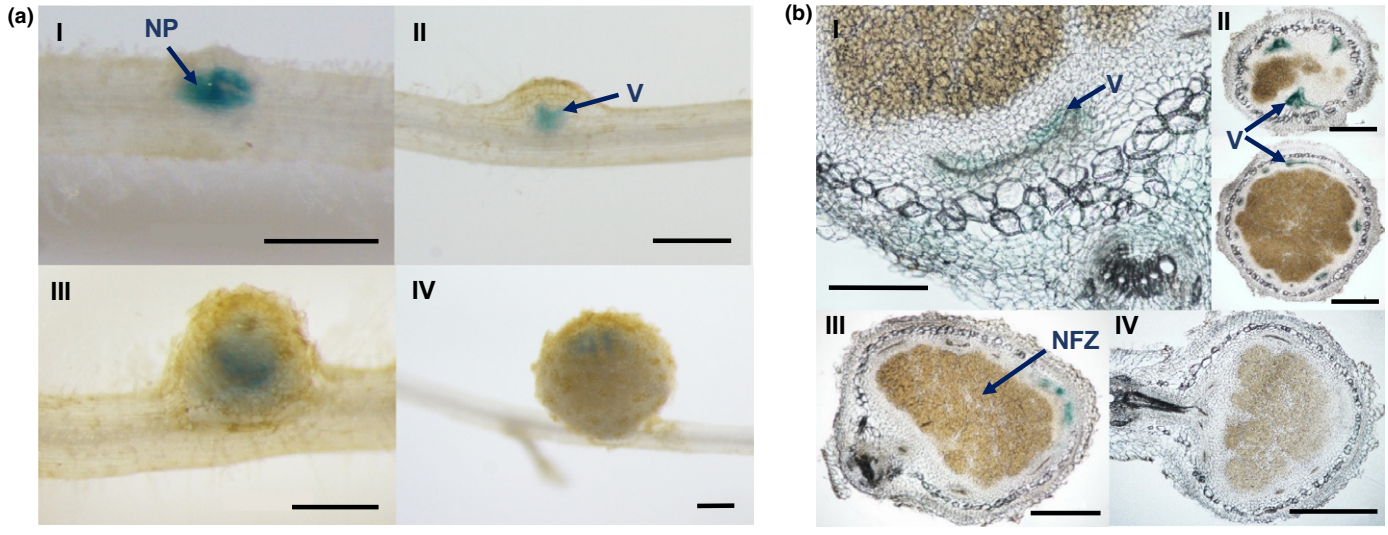

Fig. 3 Expression pattern of *GmGA2ox1a* during nodulation. (a) β-Glucuronidase (GUS) activity in soybean hairy roots carrying *GmGA2ox1a pro:GUS* construct. I–IV are root/nodule representatives at 5, 7, 10, 14 d post inoculation (dpi), respectively. (b) Cross-sections of *GmGA2ox1a pro:GUS-transformed* soybean nodules at (I–III) 12 and (IV) 14 dpi. Bar, 500 μm. NP, nodule primordia; V, vasculature; NFZ, nitrogen-fixing zone.

was applied. Expression was widely observed in the vasculature, pericycle, meristematic zone, and elongation zone (7 dpi; Fig. 4a, b). By 14 dpi, GUS activity was detected predominately in root and nodule vasculature (Fig. 4a III). These findings reveal a more versatile role for *GmGA3ox1a*, acting in both root and nodule development.

Identification of GA oxidase gene families

To better understand the nodulation-specific GA oxidase genes, we identified the complete gene families of *GA20ox*, *GA3ox*, and *GA2ox* in soybean, common bean, *L. japonicus*, *M. truncatula*, *S. lycopersicum*, and *P. andersonii* (Fig. 5) using *Arabidopsis* sequences as queries. This was achieved by sequence analyses, as well as phylogenetic and genomic environment analyses (Fig. S2a). It is common in soybean to have two copies of a gene due to a complete genome duplication event, and these duplicate genes often exhibit functional redundancy (Schmutz *et al.*, 2010). Based on our studies, *GmGA20ox1a* and *GmGA20ox1b* (Glyma.06g119100) were identified as duplicates (Fig. 5a) with a cDNA sequence similarity of 90.7%. Similarly, *GmGA3ox1a* and *GmGA3ox1b* (Glyma.13g361700; Fig. 5b) and *GmGA2ox1a* and *GmGA2ox1b* (Glyma.10g010700; Fig. 5c) were identified as duplicates, each pair sharing similarity of 94.8% and 94.6%, respectively.

Orthologues of *GmGA20ox1a*, *GmGA3ox1a*, or *GmGA2ox1a* were identified in each of the species investigated (Figs S7–S9). By contrast, no orthologous genes were identified in *Arabidopsis*, *S. lycopersicum*, or *P. andersonii*; therefore, we hypothesize that these GA oxidase genes are legume specific and evolved from a common legume ancestor. The orthologues identified for *GmGA20ox1*, *GmGA3ox1*, and *GmGA2ox1* in common bean, *L. japonicus*, and *M. truncatula* include Phvul.009G131500, Lj0g3v0308649, Lj0g3v0274439, and Medtr3g088745; Phvul.005G173500, Lj0g3v0106899, and Medtr2g102570; and Phvul.007G212200, Lj0g3v0099859, and Medtr1g086550, respectively.

Disruption of GA homeostasis impairs soybean nodulation

To further determine the role of GA homeostasis in nodule organogenesis, *GmGA20ox1a*, *GmGA3ox1a*, and *GmGA2ox1a* were subjected to constitutive overexpression and/or CRISPR/Cas9-induced gene editing in transgenic soybean hairy roots. Overexpression of *GmGA20ox1a* resulted in significantly more, but smaller, nodules compared with the EV control (Figs 6a–c, S1c), with no obvious morphological changes in the root (Fig. S1d). The nodules on these overexpressing roots exhibited retarded development (Fig. 6d), confirming a critical role for *GmGA20ox1a* in determining nodule growth. Overexpression of the GA-catabolism gene, *GmGA2ox1a*, resulted in reduced nodule numbers (Fig. 6e,f).

For CRISPR/Cas9 gene-editing studies, sgRNAs were designed to target each pair of duplicate genes (i.e. both the *a*

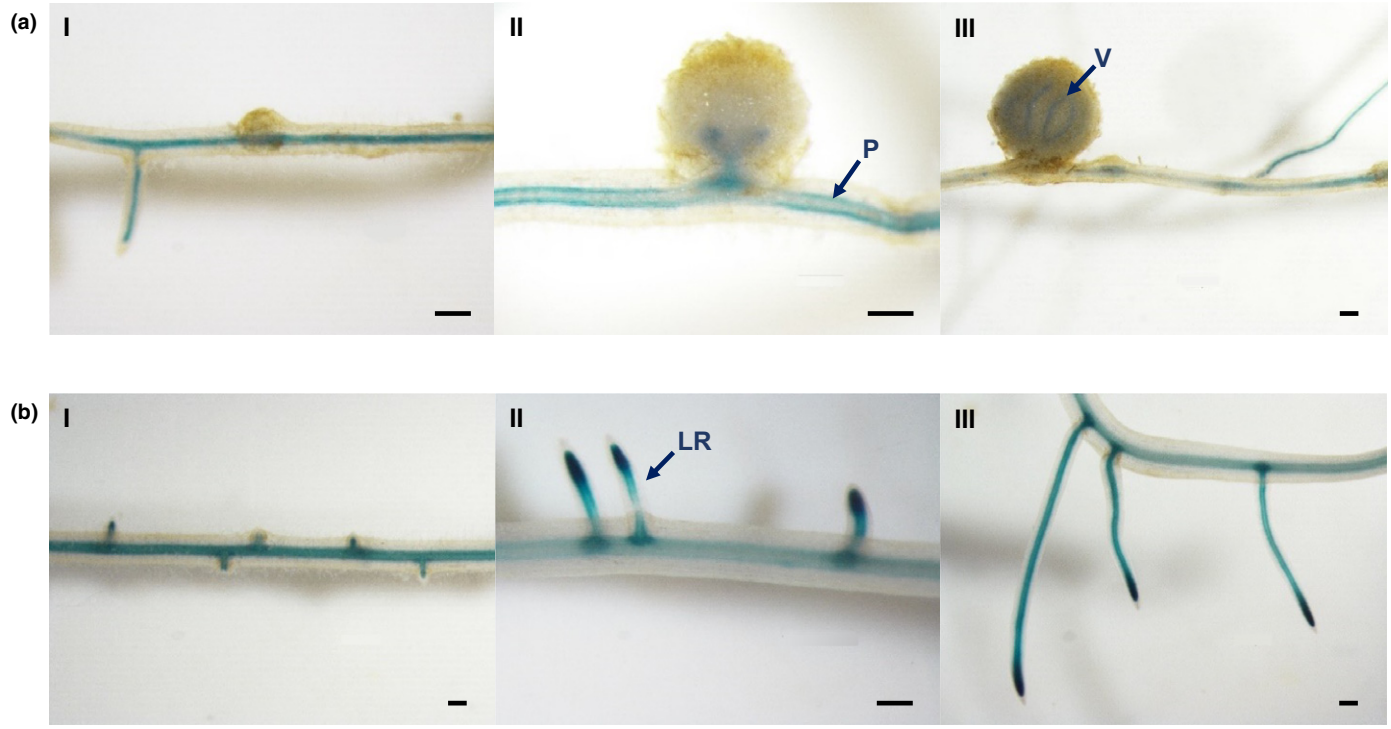

Fig. 4 Expression pattern of *GmGA3ox1a* in response to wild-type (WT) or *nodC*$^{-}$ rhizobia inoculation. (a) *GmGA3ox1a* promoter activity in soybean hairy inoculated with WT *Bradyrhizobium diazoefficiens*. I–III are root/nodule representatives at 5, 10, and 14 d post inoculation (dpi), respectively. (b) *GmGA3ox1a pro:GUS* expression in soybean hairy root inoculated with *nodC*$^{-}$ at (I–III) 5, 10, and 14 dpi, respectively. Bar, 500 μm. P, pericycle; V, vasculature; LR, lateral root.

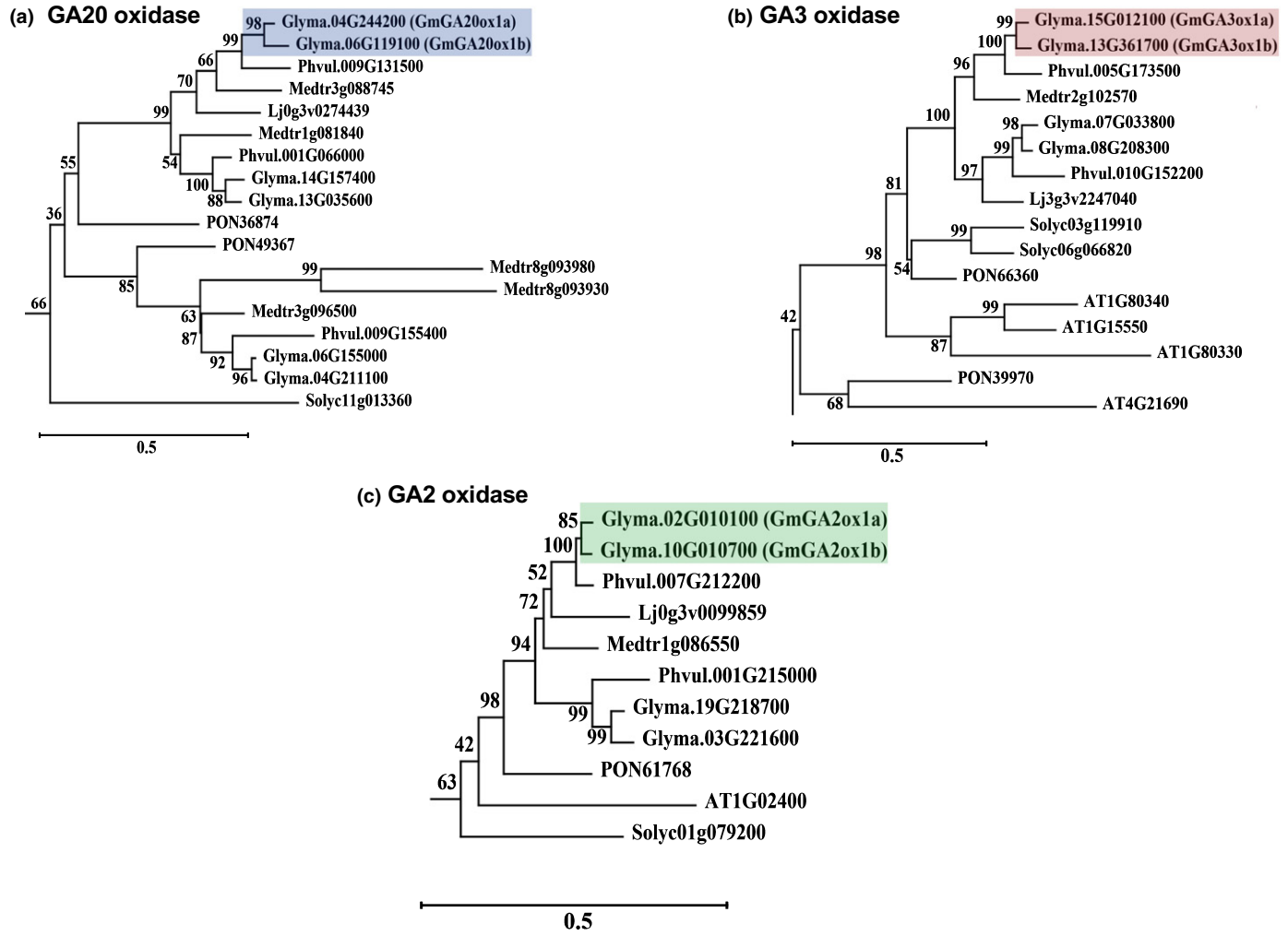

Fig. 5 Phylogenetic trees of known GA oxidases. Phylogenetic trees of (a) GA20 oxidase, (b) GA3 oxidase, and (c) GA2 oxidase of soybean, common bean, *Lotus japonicus*, *Medicago truncatula*, *Arabidopsis thaliana*, *Solanum lycopersicum*, and *Parasponia andersonii*. GA oxidase protein candidates were manually verified to contain DIOX_N (PF14226) and 2OG-FeII_Oxy (PF03171) domains. The tree is shown with bootstrap confidence values demonstrated as percentage from 1000 bootstrap replicates. Here, we present the subsets of the gene families. The full phylogenetic trees are shown in Supporting Information Figs S7–S9.

and *b* duplicate copies of *GmGA20ox1*, *GmGA3ox1*, or *GmGA2ox1*). This was done to prevent any possible redundant activity between the duplicate copies, as editing only one copy could potentially result in a compensatory effect in the expression of the other, which needed to be avoided in this experiment to determine their role in nodulation. In addition, efficacy of the CRISPR/Cas9 method used here was verified in soybean hairy roots, with sequence analysis demonstrating that indels causing frameshift mutations could be induced (Fig. 7a, with example cleavage sites shown in Fig. S2b).

CRISPR/Cas9-mediated editing of *GmGA20ox1a* and *GmGA3ox1a* significantly reduced nodule numbers (Fig. 7b). Similarly, editing of *GmGA2ox1a* also resulted in significantly fewer nodules than the control (Fig. 7b). This demonstrates that the GA content needs to be tightly regulated, as too much or too little leads to fewer nodules formed. Importantly, there was no significant phenotypic difference observed in either hairy root (Fig. 7c) or shoot development (Fig. S2c) with any of the CRISPR/Cas9 constructs tested, indicating that these genes are dispensable for hairy root or shoot growth and development, and that the changes in nodule numbers are not due to indirect effect of altered plant development (Fig. S2c,d).

Spatiotemporal distribution of bioactive GA content correlates with *GmGA20ox1a* expression

The concentration of bioactive GA was examined in developing soybean nodules using a FRET-based GPS1 (Rizza *et al.*, 2017). To determine where nodules were forming, *B. diazoefficiens* labelled with *DsRed* (M. Hayashi *et al.*, 2014) were used for visualization of the symbiotic bacteria and associated infection events.

In root tissues at 3 dpi, a relatively low level of GA was detected in root cortical cells that neighbour extending ITs (Fig. 8a,b). This could indicate that GA accumulation is not required at this stage of development and/or that it is

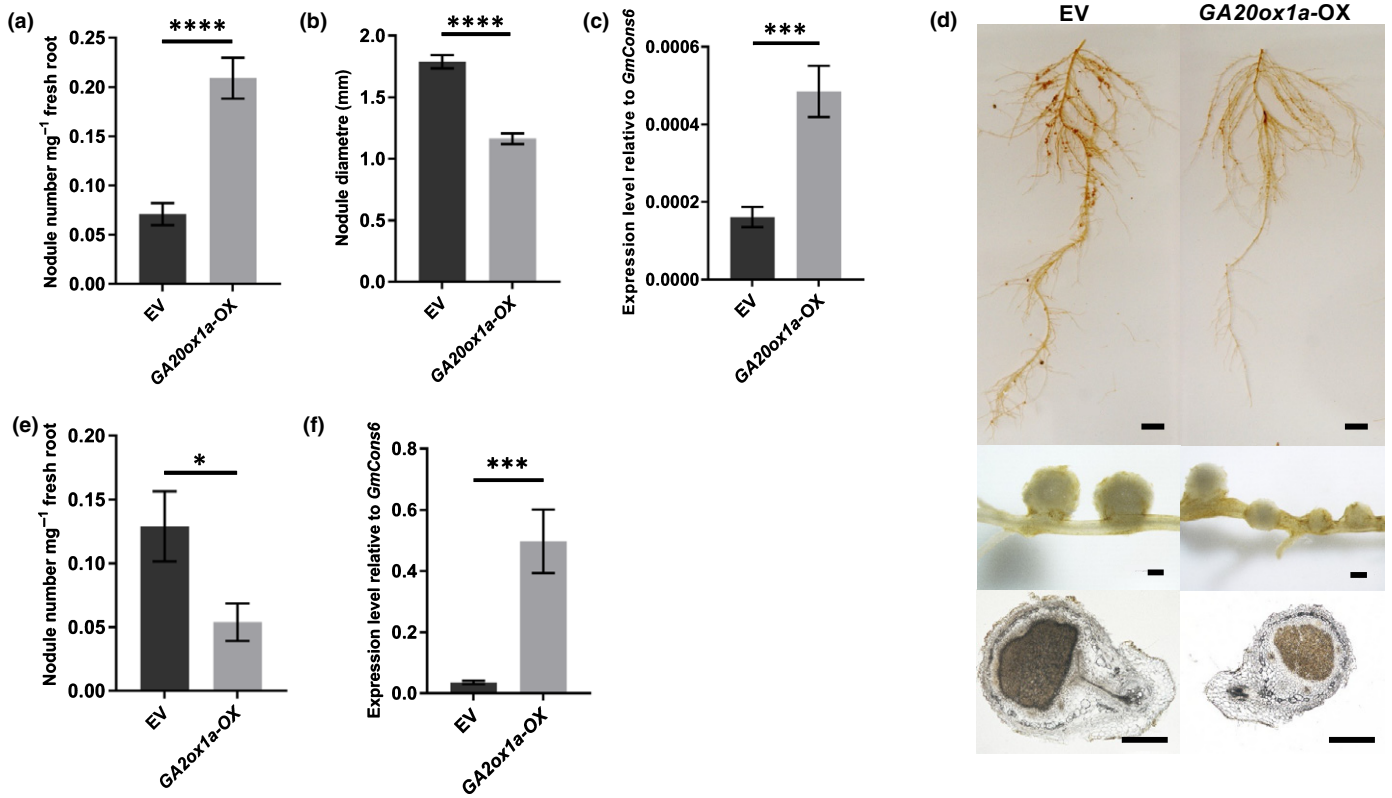

Fig. 6 Overexpression of nodule-specific GA oxidase genes. (a) Nodulation profile of individual hairy roots harbouring either empty vector (EV; $n = 3$) or *GmGA20ox1a* overexpression integrative vector (*GA20ox1a*-OX; $n = 15$) at 14 d post inoculation (dpi). (b) Nodule diameter of hairy roots transformed with EV or *GA20ox1a*-OX, 14 dpi ($n = 25$). (c) Transcript abundance of *GmGA20ox1a* in EV and *GA20ox1a*-OX transformed soybean root tissues ($n = 9$) at 14 dpi. (d) Representatives of hairy roots transformed with EV or *GA20ox1a*-OX, 14 dpi. Bars: (upper panel) 1 cm; (middle and lower panels) 500 µm. (e) Nodule number per milligram root FW and (f) *GmGA2ox1a* transcript abundance of transgenic hairy roots carrying EV ($n = 5$) or *GmGA2ox1a* overexpression binary vector (*GA2ox1a*-OX; $n = 20$), 14 dpi. Error bars indicate the SEMs (Student's *t*-test; *, $P < 0.05$; ***, $P < 0.001$; ****, $P < 0.0001$).

unfavourable for rhizobia infection progression. By 5 dpi, high GA levels were detected at the distal end of the root cortex (Fig. 8c). This is the zone where rhizobia are released into differentiating cells of soybean nodule primordia. As the nodule structure matures (7 dpi), bioactive GA was observed accumulating in actively dividing/expanding nodule cells (Fig. 8d). At this stage, the GPS1 emission ratio in outer cortical cells, where cells are actively dividing and elongating, was statistically higher than that of the infected cells (Fig. 8h,i). A similar pattern of bioactive GA accumulation was observed in emerged lateral roots (Fig. S3a), revealing a general function for GA in promoting cell division and differentiation. Interestingly, the increase in GA accumulation in the inner root cortex was exclusively observed when a nodule was forming (Fig. 8c,d) and not when a lateral root was developing (Fig. S3a). This implies that the level of bioactive GA is regulated differently in the inner root cortex in response to root and nodule primordia formation. GA accumulation was not reliably detectable at earlier stages of nodulation (e.g. 12 or 24 hpi), possibly due to any increase being localized to only a few cells at this stage of development, or that any early production of GA is quickly catabolized to sustain an optimum level of endogenous bioactive GA.

In mature nodules, the level of bioactive GA generally diminished, only remaining elevated in specific tissues (Fig. 8e–g). For example, at 12 dpi, dividing and expanding cortical cells of the nodule that are not yet enclosed by sclerenchyma cells exhibited a high level of bioactive GA (Fig. 8f). Small clusters of cells in the peripheral cell layers of the nodule also had a slightly higher GA content than surrounding tissues. No signal for bioactive GA was observed within the N-fixing zone of 14-d-old nodules (Fig. 8g). Importantly, no bioactive GA gradients were observed in transgenic hairy roots from the negative control transformed with GPS1-Not Responsive vector (GPS1-NR; Fig. S3b,c). This confirms that the observations reported here are indeed the result of biosensor activity.

Elevated GA levels block rhizobia infection and induce *GmNIN* and *GmENOD40* expression

Bioactive GA_3 and the GA inhibitor PAC were used to manipulate the GA content of the root where nodules were forming. Nodule numbers were significantly reduced in response to high concentrations ($>10^{-6}$ M) of either GA_3 or PAC (Fig. S4a–c). By contrast, lower concentrations of exogenous GA_3 (10^{-9} M) promoted nodule primordia formation (Fig. S4a). These results are consistent with previous findings that GA affects nodulation in a dose-dependent manner (Ferguson *et al.*, 2005).

To investigate the inhibitory effect of increased GA levels on nodule development, we used the supernodulating mutant

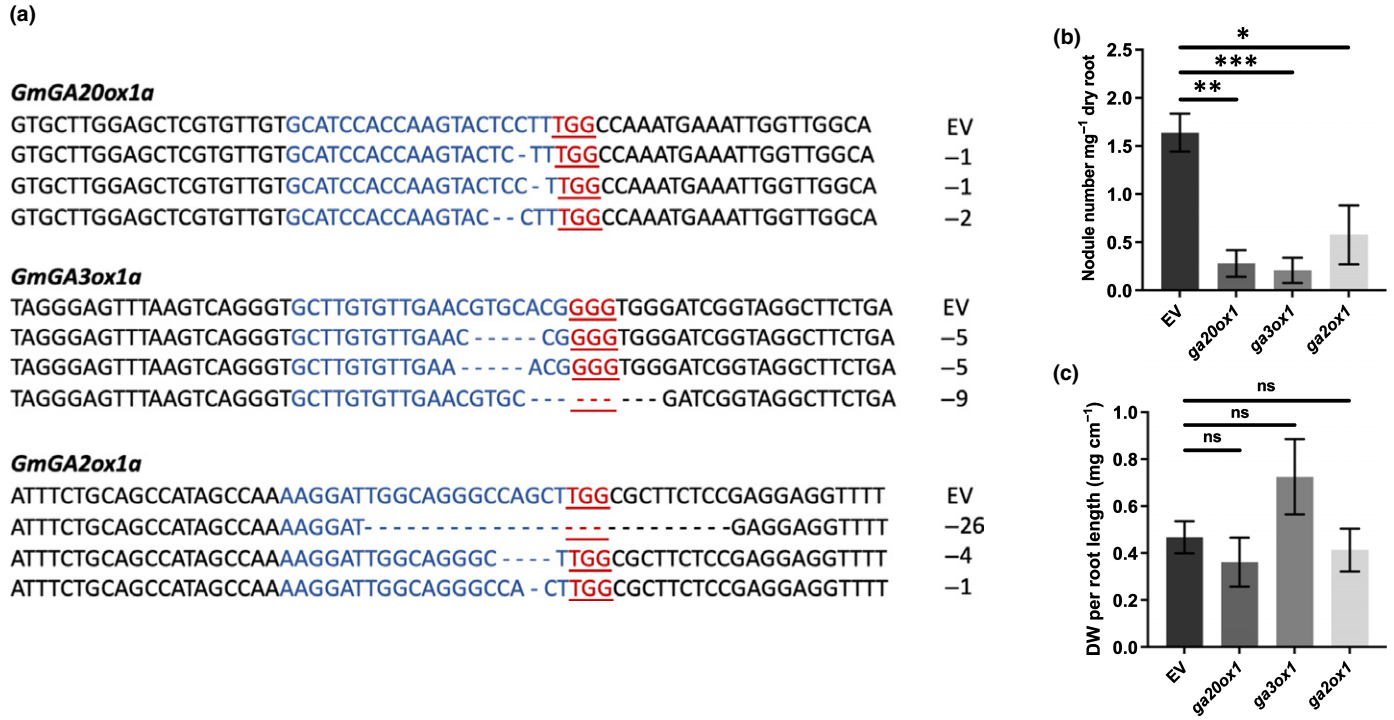

Fig. 7 CRISPR/Cas9-mediated GA oxidase gene editing. (a) Representative sequence-based mutations induced by *pCas9-GmU6-sgRNA*. Wild-type (WT) sequences of the target genes are shown with protospacer adjacent motif (NGG) sequence highlighted in red. The 20 nt single guide RNAs (sgRNAs) are shown in blue. The change in number of nucleotides is shown to the right of the targeted sequence. (b) Nodulation phenotype and (c) root weight of soybean hairy roots harbouring either empty vector (EV) or *GmGA20ox1*, *GmGA3ox1*, and *GmGA2ox1* CRISPR/Cas9 binary vectors (*ga20ox1*, *ga3ox1*, and *ga2ox1*) at 14 d post inoculation ($n \geq 6$). Nodule number is normalized by DW for individual transgenic root. Error bars indicate the SEMs. Asterisks represent significant differences when compared with the EV control (one-way ANOVA; *, $P < 0.05$; **, $P < 0.01$; ***, $P < 0.001$; ns, not significant). The experiment was repeated three times with similar results. (c) Root DW of Cas9 edited samples and the EV control. No significant differences were detected.

nts382, which has a greater proportion of ITs that progress to later stages of nodulation (Carroll *et al.*, 1985; Mathews *et al.*, 1989), with the *DsRed* expression system used here shown in Fig. S5. Application of 10^{-6} M GA_3 inhibited nodule formation in the *nts382* mutant (Fig. S4d). Multiple ITs infecting a single root hair were commonly observed for both treatments (i.e. 0 M GA_3 and 10^{-6} M GA_3; Fig. 9a–d); however, plants treated with 10^{-6} M GA_3 had significantly more ITs per infected root hair compared with the control (Fig. 9e). This might be due to GA_3 promoting IT formation or it could be the result of an adverse effect of GA_3 application on IT development triggering compensatory IT growth. GA_3 treatment also resulted in a slight increase in the length of the longest individual IT (Fig. 9f), demonstrating that GA can impact IT extension.

We also investigated the response of critical nodulation genes to GA application. *NIN* is an early nodulation gene involved in both rhizobia infection and cortical cell division (Schauser *et al.*, 1999; Soyano *et al.*, 2013; Yoro *et al.*, 2014) and acts upstream of the early nodulin gene *ENOD40* (Soyano *et al.*, 2013; Xu *et al.*, 2021). Treatments of 10^{-6} M and 10^{-4} M GA_3 significantly induced the expression of *GmNIN1a*, *GmNIN2a*, *GmNIN2b*, *GmENOD40a*, and *GmENOD40b* within 12 h of application (Fig. 10). This demonstrates that GA is sufficient to induce *NIN* and *ENOD40* expression, even in the absence of compatible rhizobia. Their expression was much higher by GA and rhizobia cotreatment (Fig. S6a). Collectively, our results demonstrate that GA can positively regulate IT elongation and IT number per root hair and induces the expression of *NIN* and *ENOD40*.

Discussion

Plant hormones, including GA, are well known for their role in legume nodule development (Ferguson & Mathesius, 2003, 2014; S. Hayashi *et al.*, 2014). Here, we provide further evidence for a critical role of GA in nodule organogenesis and demonstrate that the level of bioactive GA changes both spatially and temporally, supporting the idea that the hormone has both positive and negative roles during nodulation (Fletcher *et al.*, 1958; Thurber *et al.*, 1958; Galston, 1959; Mes, 1959; Ferguson *et al.*, 2005, 2011; Lievens *et al.*, 2005; Maekawa *et al.*, 2009; Fonouni-Farde *et al.*, 2016; McAdam *et al.*, 2018). Moreover, we demonstrate that tight regulation of the GA content is controlled by a number of GA oxidases that function in biosynthesis and catabolism of the hormone.

Using a FRET-based method for detecting bioactive GA distribution at the cellular level (Rizza *et al.*, 2017), we identified high levels of GA in early nodule development that localized to the transient nodule meristem and remained in this region until it is no longer meristematic. This partially overlaps with the cortical distribution pattern observed for cytokinin in developing determinate nodules, suggesting positive regulatory roles for these

New Phytologist

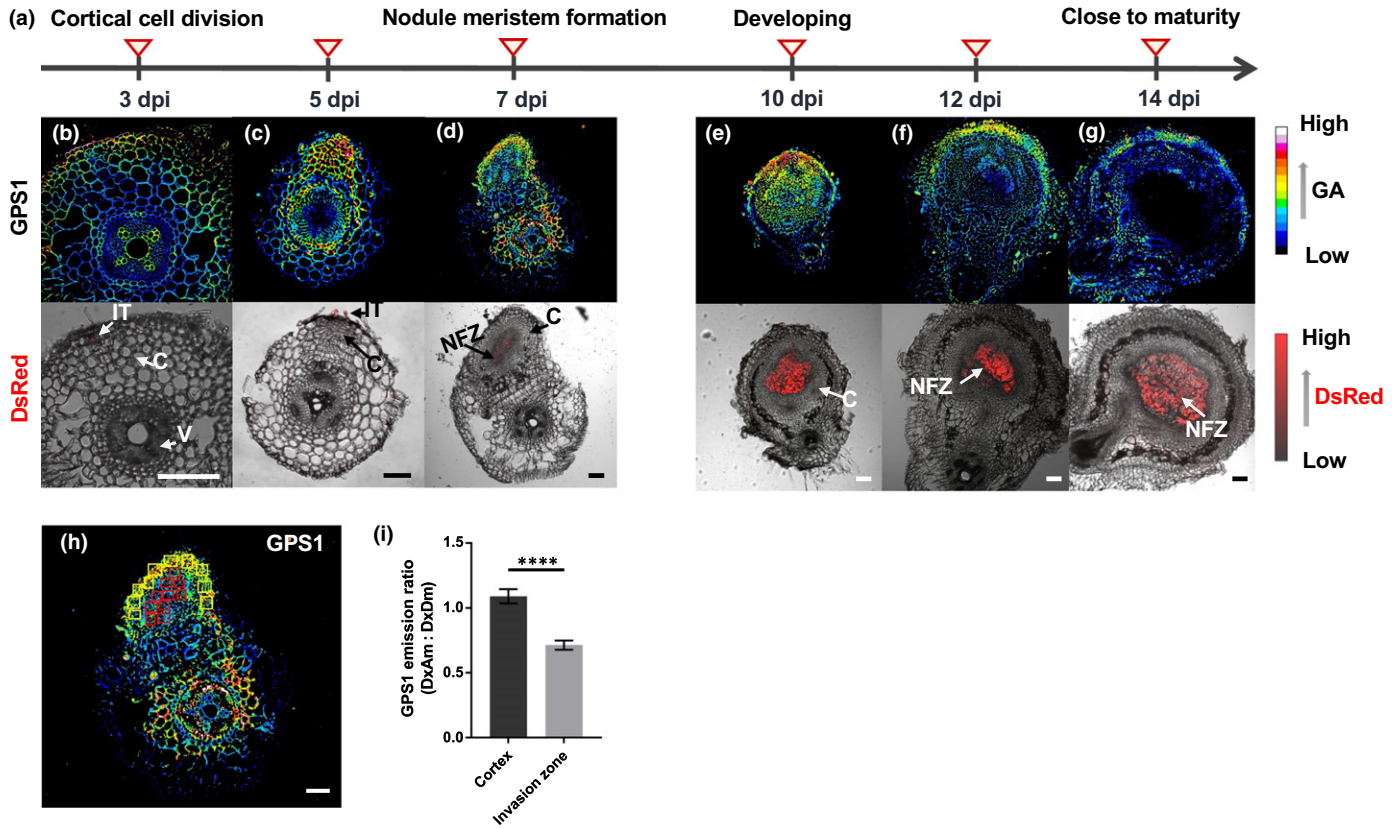

Fig. 8 Nodule development and bioactive GA gradients. (a) Timeline of physiological changes associated with nodule initiation (dpi, d post inoculation). (b–g) Two-dimensional images of Gibberellin Perception Sensor 1 (GPS1; upper panel) emission ratios and DsRed (lower panel) emission in developing soybean nodules. The GPS1 and DsRed panels are in the same scale. Bar, 100 μm. (h) Selected rectangle regions of interest for quantification of GPS1 emission ratio. Yellow and red rectangles indicate randomly selected subsection of cortex and NFZ, respectively. Bar, 100 μm. (i) Bar graph showing GPS1 emission ratio for 10 random regions from nodule cortex and N-fixing zones, respectively ($n = 10$). Error bars indicate SEMs. (Student's *t*-test; ****, $P < 0.0001$). C, cortex; V, vasculature; IT, infection thread; NFZ, nitrogen-fixing zone.

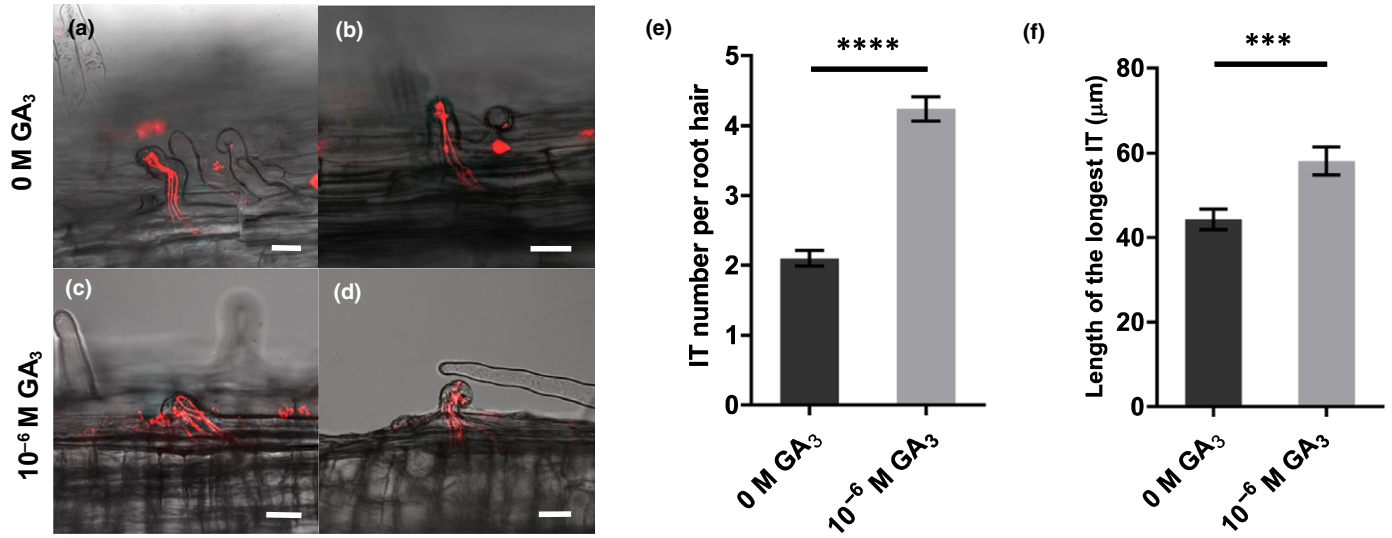

Fig. 9 Fluorescence microscopy analysis of infection thread (IT) by using *DsRed*-expressing *Bradyrhizobium diazoefficiens*. IT visualization in the roots of supernodulation mutant *nts382* inoculated with *B. diazoefficiens* expressing *DsRed* (7 d post inoculation; (a, b) 0 M GA_3; (c, d) 10^{-6} M GA_3 treated). Bar, 20 μm. The images are representatives of 50 individual infection sites of control or treatment. (e) IT numbers at individual infection sites ($n = 50$). (f) The length of the longest IT at individual IT sites ($n = 50$). Error bars indicate the SEMs. Asterisks indicate statistically significant differences between treated and control roots (Student's *t*-test; ***, $P < 0.001$; ****, $P < 0.0001$).

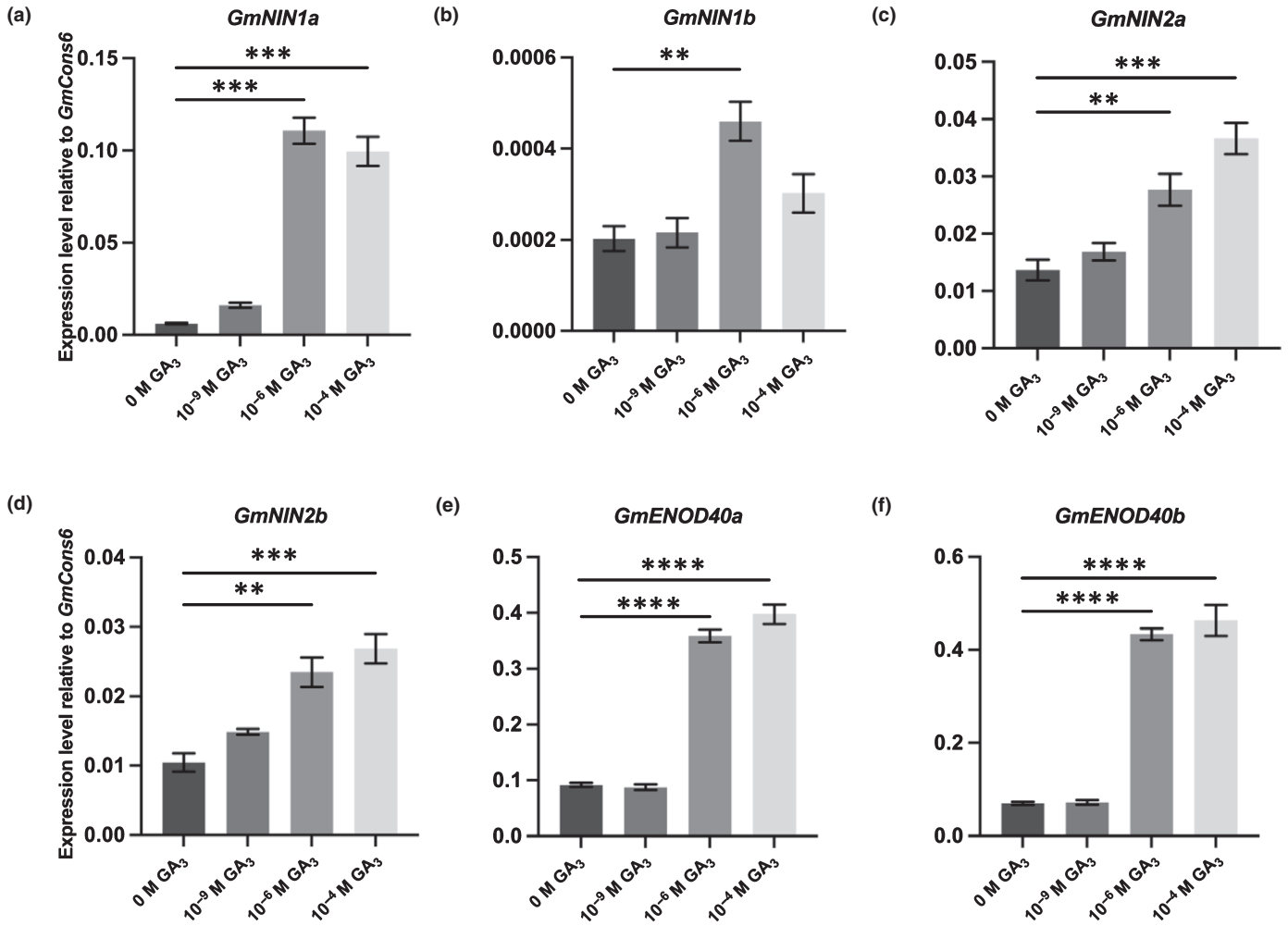

Fig. 10 Exogenous GA_3 induced early nodulation genes expression. Transcription levels of (a–d) *NIN* and (e, f) *ENOD40* in soybean cv Bragg after GA_3 treatments (12 h post inoculation). The gene duplicates were identified according to sequence similarity and gene synteny (Supporting Information Fig. S6b). *GmCons6* was employed as the housekeeping gene. Control roots were not treated with GA solutions. Error bars indicate the SEMs resulting from three biological controls. Asterisks indicate statistically significant differences between treated and control roots (one-way ANOVA; **, $P < 0.01$; ***, $P < 0.001$; ****, $P < 0.0001$).

hormones in nodule formation (Reid *et al.*, 2016; Fisher *et al.*, 2018). GAs have long been associated with similar tissues and cell types in other regions of the plant, and it is likely that the hormone has a similar role in controlling cell development and elongation during nodule formation (Stowe & Yamaki, 1957; Sachs, 1965; Cosgrove & Sovonick-Dunford, 1989; S. Hayashi *et al.*, 2014; Hedden & Sponsel, 2015; Hedden, 2020). This is further supported by mutant studies and hormone/inhibitor application assays reporting that too much or too little GA can lead to aberrant formation of the nodule structure (Ferguson *et al.*, 2005, 2011; reviewed in S. Hayashi *et al.*, 2014). Our findings suggest that application of specific concentrations of GA or PAC, or overexpression or genome editing of GA biosynthesis genes, can alter nodule number or morphology in soybean are also consistent with these results.

Using a transcriptomic and RT-qPCR approach reported in Hayashi *et al.* (2012), we identified a subset of GA oxidase genes that are significantly upregulated in response to inoculation with compatible rhizobia. This includes *GmGA20ox1a*, *GmGA3ox1a*, and *GmGA2ox1a* and their respective duplicates (Fig. 1; Table S4). However, the RNA-seq data (Table S4) indicate only the *a* copies were significantly expressed in response to competent rhizobia inoculation at 48 hpi. Therefore, for promoter-fusion and overexpression studies, we focused on the *a* copies. Promoter:GUS reporter fusion studies demonstrated that *GmGA20ox1a* and *GA2ox1a* are exclusively activated in developing nodules, whereas *GmGA3ox1a* is active in both roots and nodules, suggesting it is not nodule specific in its expression and appears to have a more extensive role in both root and nodule development. A lag in the appearance of GUS activity between the *GA20ox1a* and *GA2ox1a* promoter constructs aligns with the RT-qPCR data. This indicates that, in addition to an increased level of GA being required to maintain the transient meristem, an initial surge of GA is essential early in the process. This could be a trigger for cells in preparation for them switching from being a root cell into a nodule cell, or it could be a requirement for rhizobia recognition and/or initial infection.

The promoter activity pattern of *GmGA20ox1a* precisely overlapped with the localization and timing of bioactive GA accumulation. This also mirrors the location and timing of the transient meristem of developing soybean nodules (Newcomb *et al.*, 1979; Turgeon & Bauer, 1982; Calvert *et al.*, 1984). These findings indicate that upregulation of *GmGA20ox1a* results in an elevated GA content that is required for the persistence of the transient meristem of determinate nodules. Consistent with our findings, Lievens *et al.* (2005) also reported a *GA20ox* gene expressed in this region of developing *S. rostrata* nodules. A positive role of bioactive GA was also found in maintaining pea meristem functioning (Serova *et al.*, 2019).

Interestingly, an exception to the overlap between *GmGA20ox1a* expression and bioactive GA accumulation is in the root vasculature (i.e. at 5–7 dpi). This might be a reflection of enhanced *GA2ox1a* expression in this region. Indeed, as the nodule develops, *GmGA2ox1a* expression is restricted to the nodule vasculature. GA such as GA_{20}, the direct precursor of bioactive GA_1, has been shown to be transported systemically within the plant and can be degraded by GA2ox (Hedden & Kamiya, 1997; Yamaguchi, 2008). Therefore, the expression of *GmGA2ox1a* around the vasculature could indicate its role in degrading bioactive GA to prevent it from being transported out. This would inadvertently impact aspects of plant development outside the intended nodule. In fact, *GmGA2ox1a* activity became nearly undetectable in mature nodules when the level of bioactive GA diminishes and GA catabolism would presumably no longer be required.

Each of *GmGA20ox1a*, *GmGA3ox1a*, and *GmGA2ox1a* were confirmed to have a role in the nodulation process through functional characterization studies. Bioinformatic and phylogenetic analyses revealed that *GA20ox1a* and *GA2ox1a* do not have an orthologue in *Arabidopsis*, tomato, or *P. andersonii* (the non-legume species that is capable of forming nodules), suggesting they are unique to legumes and evolved in an early ancestor via neofunctionalization of a related gene family member. CRISPR/Cas9-mediated gene editing of each resulted in fewer nodules formed (Figs 7b, S2e). This further demonstrates that too much bioactive GA (caused by editing *GmGA2ox1a*) or too little (caused by editing *GmGA20ox1a* or *GmGA3ox1a*) can impair nodule organogenesis. Similarly, overexpression of *GA2ox1a*, which would lead to an increased level of bioactive GA, also resulted in fewer nodules formed. By contrast, overexpression of *GA20ox1a* resulted in a slight increase in nodule numbers. Collectively, these findings are consistent with GA application studies in pea (Ferguson *et al.*, 2005, 2011), *S. rostrata* (Lievens *et al.*, 2005), *L. japonicus* (Maekawa *et al.*, 2009), and soybean (here), where a low concentration of GA promote nodulation but higher concentrations inhibit it. They are also consistent with studies in pea GA mutants where an altered GA content increased or reduced the number of nodules formed (Ferguson *et al.*, 2005, 2011). Together, the results agree with previous conclusions that a specific level of GA is required for optimum nodule development and that this level differs between tissue types and at different stages of the nodulation process (Ferguson *et al.*, 2005, 2011; reviewed in S. Hayashi *et al.*, 2014).

The findings herein would be expected if GA is acting in cell division and elongation. A slight increase in the level of GA could promote nodule development by enhancing cells to divide, differentiate, and elongate (Kawaguchi *et al.*, 1996; Lievens *et al.*, 2005; Hayashi *et al.*, 2012). By contrast, higher GA levels might inhibit these processes by elevating ethylene production (Ferguson *et al.*, 2011). Alternatively, GA might influence rhizobia invasion and/or IT development and progression as demonstrated here, and this could impact positively or negatively on nodule numbers, depending on the GA concentration and stage of nodule development. Fine-tuning could also result from feedforward (Elliott *et al.*, 2001) and feedback (Yamaguchi *et al.*, 2014) mechanisms that function to control GA homeostasis.

Relatively low GA signal was captured in cells adjacent to ITs, suggesting a negative regulatory role of GA during rhizobia infection. Previous studies revealed that GA negatively regulates root hair deformation and infection events (Maekawa *et al.*, 2009; McAdam *et al.*, 2018) via a DELLA-dependent mechanism (Fonouni-Farde *et al.*, 2016; Jin *et al.*, 2016). Multiple ITs in a single root hair have previously been reported for several legume species (Turgeon & Bauer, 1982, 1985; Gage *et al.*, 1996; Gage, 2002; Liu *et al.*, 2019). Interestingly, we found that treatment of 10^{-6} M GA_3 increased the number of ITs per root hair in soybean. This might be due to GA enhancing the formation of ITs (Callaham & Torrey, 1981; Turgeon & Bauer, 1985). Alternatively, exogenous GA might obstruct IT development, resulting in a feedforward mechanism where additional ITs are formed to enhance the chance of success for progression towards the cortex. Ferguson *et al.* (2011) reported that double mutants of GA biosynthesis and autoregulation of nodulation (AON) mutants exhibit a supernodulation phenotype with nodules that are abnormal. This indicates that GA likely acts independently of AON. Therefore, the GA-related IT development is less likely to be affected by AON.

Our findings also revealed that *NIN* and *ENOD40*, essential genes involved in nodulation, were significantly upregulated by GA_3 application regardless of the presence of compatible rhizobia. This is consistent with previous studies reporting that GA can promote nodule formation (Kawaguchi *et al.*, 1996; Akamatsu *et al.*, 2021) and suggests that GA acts through *NIN* and *ENOD40* in the nodulation molecular pathway. Indeed, Akamatsu *et al.* (2021) recently identified a GA-responsive *cis*-acting region in the promotor of NIN that regulates for nodule formation. *GmNIN1a*, *GmNIN2a*, *GmNIN2b*, *GmENOD40a*, and *GmENOD40b* were all induced within 12 h of GA_3 application. *GmNIN1b* was also upregulated, but it was expressed at a very low level (< 100 times that of *GmNIN1a*) after either GA_3 or rhizobia treatment, suggesting it is not likely as biologically relevant. Previous reports have demonstrated that epidermal-expressed *NIN* promotes infection, whereas cortical-expressed *NIN* inhibits it (Murray *et al.*, 2007; Yoro *et al.*, 2014; Fournier *et al.*, 2015; Vernié *et al.*, 2015). Future studies aimed at understanding cell-specific *NIN* expression in response to GA and rhizobia will be of great interest to pursue.

We functionally characterized three GA oxidase genes and their duplicates acting in soybean nodulation and established the pattern of bioactive GA localization during nodule development.

We also developed a novel strain of *B. diazoefficiens* that constitutively expresses the *DsRed* reporter gene, and we used this to visualize infection and nodule occupancy and to help establish how GA impacts on these processes. Our results show that tight control over the availability of bioactive GA is critical for successful nodule development with a positive correlation between GA accumulation and nodule primordium establishment. Future studies that advance our knowledge of how GA impacts rhizobia infection and nitrogen fixation, including any involvement of rhizobia produced GAs (S. Hayashi *et al.* 2014; Hershey *et al.*, 2014; Nett *et al.*, 2017), will further enhance this understanding.

Acknowledgements

This work was funded by Australian Research Council Discovery Project grants to BJF and PMG (DP130102266, DP130103084, and DP190102996). XC thanks the China Scholarship Council (CSC NO.201506300101) and the University of Queensland for scholarship support. We thank Dr Yosuke Umehara (Institute of Agrobiological Sciences, National Agriculture and Food Research Organization, Japan) for providing *pBjGroESL4::DsRed2*, Dr Alexander M. Jones (Sainsbury Laboratory, Cambridge University, Cambridge, UK) for providing *p16-nlsGPS1* and *p16-nlsGPS1-NR*, and Prof. Yajun Xi (College of Agronomy, Northwest A&F University, Yangling, China) for providing *pCas9-GmU6-sgRNA*. We are grateful to *Plant Biotechnology Journal* for permission to reproduce aspects of Fig. 5 from Hayashi *et al.* (2012). We would also like to thank Dr Mengbai Zhang, Dr April Hastwell, Kerry Vinall, and Katy Carroll for their technical assistance. Lastly, we would like to sincerely thank the three reviewers who contributed their time, effort, and expertise to help improve this article.

Author contributions

XC, BJF and PMG designed the project; XC and HS performed the experiments and analyzed the data with BJF; XC and BJF drafted the manuscript; SH contributed Fig. 1. All authors edited the manuscript.

ORCID

Xitong Chu https://orcid.org/0000-0002-3378-3422
Brett J. Ferguson https://orcid.org/0000-0003-3737-8368
Peter M. Gresshoff https://orcid.org/0000-0003-0693-2813
Satomi Hayashi https://orcid.org/0000-0002-2468-713X
Huanan Su https://orcid.org/0000-0002-7714-2141

Data availability

The data that support the findings of this study are available from the corresponding author upon reasonable request.

References

Akamatsu A, Nagae M, Nishimura Y, Montero DR, Ninomiya S, Kojima M, Takebayashi Y, Sakakibara H, Kawaguchi M, Takeda N. 2021. Endogenous gibberellins affect root nodule symbiosis via transcriptional regulation of *NODULE INCEPTION* in *Lotus japonicus*. *The Plant Journal* **105**: 1507–1520.

Brinkman EK, Chen T, Amendola M, van Steensel B. 2014. Easy quantitative assessment of genome editing by sequence trace decomposition. *Nucleic Acids Research* **42**: e168.

Broughton WJ, Dilworth MJ. 1971. Control of leghaemoglobin synthesis in snake beans. *Biochemical Journal* **125**: 1075–1080.

Callaham DA, Torrey JG. 1981. The structural basis for infection of root hairs of *Trifolium repens* by *Rhizobium*. *Canadian Journal of Botany* **59**: 1647–1664.

Calvert HE, Pence MK, Pierce M, Malik NS, Bauer WD. 1984. Anatomical analysis of the development and distribution of *Rhizobium* infections in soybean roots. *Canadian Journal of Botany* **62**: 2375–2384.

Carroll BJ, McNeil DL, Gresshoff PM. 1985. A supernodulation and nitrate-tolerant symbiotic (*nts*) soybean mutant. *Plant Physiology* **78**: 34–40.

Corcilius L, Hastwell AH, Zhang M, Williams J, Mackay JP, Gresshoff PM, Ferguson BJ, Payne RJ. 2017. Arabinosylation modulates the growth-regulating activity of the peptide hormone CLE40a from soybean. *Cell Chemical Biology* **24**: 1347–1355.

Cosgrove DJ, Sovonick-Dunford SA. 1989. Mechanism of gibberellin-dependent stem elongation in peas. *Plant Physiology* **89**: 184–191.

Coutu C, Brandle J, Brown D, Brown K, Miki B, Simmonds J, Hegedus DD. 2007. pORE: a modular binary vector series suited for both monocot and dicot plant transformation. *Transgenic Research* **16**: 771–781.

Ditta G, Stanfield S, Corbin D, Helinski DR. 1980. Broad host range DNA cloning system for Gram-negative bacteria: construction of a gene bank of *Rhizobium meliloti*. *Proceedings of the National Academy of Sciences, USA* **77**: 7347–7351.

Elliott RC, Ross JJ, Smith JJ, Lester DR, Reid JB. 2001. Feed-forward regulation of gibberellin deactivation in pea. *Journal of Plant Growth Regulation* **20**: 87–94.

Ferguson BJ, Foo E, Ross JJ, Reid JB. 2011. Relationship between gibberellin, ethylene and nodulation in *Pisum sativum*. *New Phytologist* **189**: 829–842.

Ferguson BJ, Indrasumunar A, Hayashi S, Lin MH, Lin YH, Reid DE, Gresshoff PM. 2010. Molecular analysis of legume nodule development and autoregulation. *Journal of Integrative Plant Biology* **52**: 61–76.

Ferguson BJ, Mathesius U. 2003. Signaling interactions during nodule development. *Journal of Plant Growth Regulation* **22**: 47–72.

Ferguson BJ, Mathesius U. 2014. Phytohormone regulation of legume–rhizobia interactions. *Journal of Chemical Ecology* **40**: 770–790.

Ferguson BJ, Ross JJ, Reid JB. 2005. Nodulation phenotypes of gibberellin and brassinosteroid mutants of pea. *Plant Physiology* **138**: 2396–2405.

Fisher J, Gaillard P, Fellbaum CR, Subramanian S, Smith S. 2018. Quantitative 3D imaging of cell level auxin and cytokinin response ratios in soybean roots and nodules. *Plant, Cell & Environment* **41**: 2080–2092.

Fletcher WW, Alcorn JWS, Raymond JC. 1958. Effect of gibberellic acid on the nodulation of white clover (*Trifolium repens* L.). *Nature* **182**: 1319–1320.

Fonouni-Farde C, Kisiala A, Brault M, Emery RN, Diet A, Frugier F. 2017. DELLA1-gibberellin signaling regulates cytokinin-dependent symbiotic nodulation. *Plant Physiology* **175**: 1795–1806.

Fonouni-Farde C, Tan S, Baudin M, Brault M, Wen J, Mysore KS, Niebel A, Frugier F, Diet A. 2016. DELLA-mediated gibberellin signalling regulates Nod factor signalling and rhizobial infection. *Nature Communications* **7**: e12636.

Fournier J, Teillet A, Chabaud M, Ivanov S, Genre A, Limpens E, de Carvalho-Niebel F, Barker DG. 2015. Remodeling of the infection chamber before infection thread formation reveals a two-step mechanism for rhizobial entry into the host legume root hair. *Plant Physiology* **167**: 1233–1242.

Gage DJ. 2002. Analysis of infection thread development using Gfp and DsRed-expressing *Sinorhizobium meliloti*. *Journal of Bacteriology* **184**: 7042–7046.

Gage DJ, Bobo T, Long SR. 1996. Use of green fluorescent protein to visualize the early events of symbiosis between *Rhizobium meliloti* and alfalfa (*Medicago sativa*). *Journal of Bacteriology* **178**: 7159–7166.

Galston AW. 1959. Gibberellins and nodulation. *Nature* **183**: 545.

Harberd NP, Belfield E, Yasumura Y. 2009. The angiosperm gibberellin-GID1-DELLA growth regulatory mechanism: how an 'inhibitor of an inhibitor' enables flexible response to fluctuating environments. *Plant Cell* **21**: 1328–1339.

Hayashi M, Shiro S, Kanamori H, Mori-Hosokawa S, Sasaki-Yamagata H, Sayama T, Nishioka M, Harada K, Kouchi H, Saeki Y *et al.* 2014. A thaumatin-like protein, Rj4, controls nodule symbiotic specificity in soybean. *Plant Cell Physiology* **55**: 1679–1689.

Hayashi S, Gresshoff PM, Ferguson BJ. 2014. Mechanistic action of gibberellins in legume nodulation. *Journal of Integrative Plant Biology* **56**: 971–978.

Hayashi S, Reid DE, Lorenc MT, Stiller JD, Edwards D, Gresshoff PM, Ferguson BJ. 2012. Transient Nod factor-dependent gene expression in the nodulation-competent zone of soybean (*Glycine max* [L.] Merr.) roots. *Plant Biotechnology Journal* **10**: 995–1010.

Hedden P. 2020. The current status of research on gibberellin biosynthesis. *Plant Cell Physiology* **61**: 1832–1849.

Hedden P, Kamiya Y. 1997. Gibberellin biosynthesis: enzymes, genes and their regulation. *Annual Review of Plant Physiology and Plant Molecular Biology* **48**: 431–460.

Hedden P, Sponsel V. 2015. A century of gibberellin research. *Journal of Plant Growth Regulation* **34**: 740–760.

Hershey DM, Lu X, Zi J, Peters RJ. 2014. Functional conservation of the capacity for *ent*-kaurene biosynthesis and an associated operon in certain rhizobia. *Journal of Bacteriology* **196**: 100–106.

Jefferson RA, Kavanagh TA, Bevan MV. 1987. GUS fusions: beta-glucuronidase as a sensitive and versatile gene fusion marker in higher plants. *EMBO Journal* **6**: 3901–3907.

Jin Y, Liu H, Luo D, Yu N, Dong W, Wang C, Zhang X, Dai H, Yang J, Wang E. 2016. DELLA proteins are common components of symbiotic rhizobial and mycorrhizal signalling pathways. *Nature Communications* **7**: e12433.

Kawaguchi M, Imaizumi-Anraku H, Fukai S, Syono K. 1996. Unusual branching in the seedlings of *Lotus japonicus-gibberellins* reveal the nitrogen-sensitive cell divisions within the pericycle on roots. *Plant and Cell Physiology* **37**: 461–470.

Kereszt A, Li D, Indrasumunar A, Nguyen CD, Nontachaiyapoom S, Kinkema M, Gresshoff PM. 2007. *Agrobacterium rhizogenes-mediated* transformation of soybean to study root biology. *Nature Protocols* **2**: 948–952.

Kim GB, Son SU, Yu HJ, Mun JM. 2019. *MtGA2ox10* encoding C20-GA2-oxidase regulates rhizobial infection and nodule development in *Medicago truncatula*. *Scientific Reports* **9**: e5952.

Libault M, Thibivilliers S, Bilgin DD, Radwan O, Benitez M, Clough SJ, Stacey G. 2008. Identification of four soybean reference genes for gene expression normalization. *Plant Genome* **1**: 44–54.

Lievens S, Goormachtig S, Den Herder J, Capoen W, Mathis R, Hedden P, Holsters M. 2005. Gibberellins are involved in nodulation of *Sesbania rostrata*. *Plant Physiology* **139**: 1366–1379.

Lin J, Frank M, Reid D. 2020. No home without hormones: how plant hormones control legume nodule organogenesis. *Plant Communications* **1**: e100104.

Liu C-W, Breakspear A, Stacey N, Findlay K, Nakashima J, Ramakrishnan K, Liu M, Xie F, Endre G, de Carvalho-Niebel F *et al.* 2019. A protein complex required for polar growth of rhizobial infection threads. *Nature Communications* **10**: e2848.

Maekawa T, Maekawa-Yoshikawa M, Takeda N, Imaizumi-Anraku H, Murooka Y, Hayashi M. 2009. Gibberellin controls the nodulation signaling pathway in *Lotus japonicus*. *The Plant Journal* **58**: 183–194.

Mathews A, Carroll BJ, Gresshoff PM. 1989. Development of *Bradyrhizobium infections* in supernodulating and non-nodulating mutants of soybean (*Glycine max* [L.] Merrill). *Protoplasma* **150**: 40–47.

McAdam EL, Reid JB, Foo E. 2018. Gibberellins promote nodule organogenesis but inhibit the infection stages of nodulation. *Journal of Experimental Botany* **69**: 2117–2130.

Mes MG. 1959. Influence of gibberellic acid and photoperiod on the growth, flowering, nodulation and nitrogen assimilation of *Vicia villosa*. *Nature* **184**: 2035–2036.

Mun T, Bachmann A, Gupta V, Stougaard J, Andersen SU. 2016. Lotus Base: an integrated information portal for the model legume *Lotus japonicus*. *Scientific Reports* **6**: e39447.

Murase K, Hirano Y, Sun TP, Hakoshima T. 2008. Gibberellin-induced DELLA recognition by the gibberellin receptor GID1. *Nature* **456**: 459–463.

Murray JD, Karas BJ, Sato S, Tabata S, Amyot L, Szczyglowski K. 2007. A cytokinin perception mutant colonized by *Rhizobium* in the absence of nodule organogenesis. *Science* **315**: 101–104.

Nett RS, Contreras T, Peters RJ. 2017. Characterization of CYP115 as a gibberellin 3-oxidase indicates that certain rhizobia can produce bioactive gibberellin A4. *ACS Chemical Biology* **12**: 912–917.

Newcomb W, Sippell D, Peterson RL. 1979. The early morphogenesis of *Glycine max* and *Pisum sativum* root nodules. *Canadian Journal of Botany* **57**: 2603–2616.

Nieuwkoop AJ, Banfalvi ZS, Deshmane N, Gerhold D, Schell MG, Sirotkin KM, Stacey G. 1987. A locus encoding host range is linked to the common nodulation genes of *Bradyrhizobium japonicum*. *Journal of Bacteriology* **169**: 231–2638.

Reid DE, Heckmann AB, Novák O, Kelly S, Stougaard J. 2016. CYTOKININ OXIDASE/DEHYDROGENASE3 maintains cytokinin homeostasis during root and nodule development in *Lotus japonicus*. *Plant Physiology* **170**: 1060–1074.

Rizza A, Walia A, Lanquar V, Frommer WB, Jones AM. 2017. *In vivo* gibberellin gradients visualized in rapidly elongating tissues. *Nature Plants* **3**: 803–813.

Rizza A, Walia A, Tang B, Jones AM. 2019. Visualizing cellular gibberellin levels using the nlsGPS1 Förster resonance energy transfer (FRET) biosensor. *JoVE* **143**: e58739.

Sachs RM. 1965. Stem elongation. *Annual Review of Plant Physiology* **16**: 73–96.

Sato S, Nakamura Y, Kaneko T, Asamizu E, Kato T, Nakao M, Sasamoto S, Watanabe A, Ono A, Kawashima K *et al.* 2008. Genome structure of the legume, *Lotus japonicus*. *DNA Research* **15**: 227–239.

Schauser L, Roussis A, Stiller J, Stougaard J. 1999. A plant regulator controlling development of symbiotic root nodules. *Nature* **402**: 191–195.

Schmutz J, Cannon SB, Schlueter J, Ma J, Mitros T, Nelson W, Hyten DL, Song Q, Thelen JJ, Cheng J *et al.* 2010. Genome sequence of the paleopolyploid soybean. *Nature* **463**: 178–183.

Schmutz J, McClean PE, Mamidi S, Wu GA, Cannon SB, Grimwood J, Jenkins J, Shu S, Song Q, Chavarro C *et al.* 2014. A reference genome for common bean and genome-wide analysis of dual domestications. *Nature Genetics* **46**: 707–713.

Serova TA, Tsyganova AV, Tikhonovich IA, Tsyganov VE. 2019. Gibberellins inhibit nodule senescence and stimulate nodule meristem bifurcation in pea (*Pisum sativum* L.). *Frontiers in Plant Science* **10**: e285.

Silverstone AL, Ciampaglio CN, Sun TP. 1998. The *Arabidopsis RGA* gene encodes a transcriptional regulator repressing the gibberellin signal transduction pathway. *Plant Cell* **10**: 155–169.

Soyano T, Kouchi H, Hirota A, Hayashi M. 2013. Nodule inception directly targets *NF-Y* subunit genes to regulate essential processes of root nodule development in *Lotus japonicus*. *PLoS Genetics* **9**: e1003352.

Stowe BB, Yamaki T. 1957. The history and physiological action of the gibberellins. *Annual Review of Plant Physiology* **8**: 181–216.

Sun TP. 2011. The molecular mechanism and evolution of the GA-GID1-DELLA signaling module in plants. *Current Biology* **21**: R338–R345.

Sun X, Hu Z, Chen R, Jiang Q, Song G, Zhang H, Xi Y. 2015. Targeted mutagenesis in soybean using the CRISPR-Cas9 system. *Scientific Reports* **5**: e10342.

Tang H, Krishnakumar V, Bidwell S, Rosen B, Chan A, Zhou S, Gentzbittel L, Childs KL, Yandell M, Gundlach H *et al.* 2014. An improved genome release (version Mt4. 0) for the model legume *Medicago truncatula*. *BMC Genomics* **15**: 1–14.

Thurber GA, Douglas JR, Galston AW. 1958. Inhibitory effect of gibberellins on nodulization in dwarf beans, *Phaseolus vulgaris*. *Nature* **181**: 1082–1083.

Tomato Genome Consortium. 2012. The tomato genome sequence provides insights into fleshy fruit evolution. *Nature* **485**: 635–641.

Turgeon BG, Bauer WD. 1982. Early events in the infection of soybean by *Rhizobium japonicum*. Time course and cytology of the initial infection process. *Canadian Journal of Botany* **60**: 152–161.

Turgeon BG, Bauer WD. 1985. Ultrastructure of infection-thread development during the infection of soybean by *Rhizobium japonicum*. *Planta* **163**: 328–349.

Ueguchi-Tanaka M, Ashikari M, Nakajima M, Itoh H, Katoh E, Kobayashi M, Chow T-Y, Hsing Y-IE C, Kitano H, Yamaguchi I *et al.* 2005. *GIBBERELLIN INSENSITIVE DWARF1* encodes a soluble receptor for gibberellin. *Nature* **437**: 693–698.

van Velzen R, Holmer R, Bu F, Rutten L, van Zeijl A, Liu W, Santuari L, Cao Q, Sharma T, Shen D *et al.* 2018. Comparative genomics of the nonlegume *Parasponia* reveals insights into evolution of nitrogen-fixing rhizobium symbioses. *Proceedings of the National Academy of Sciences, USA* **115**: E4700–E4709.

Vernié T, Kim J, Frances L, Ding Y, Sun J, Guan D, Niebel A, Gifford ML, Carvalho-Niebel F, Oldroyd GED. 2015. The NIN transcription factor coordinates diverse nodulation programs in different tissues of the *Medicago truncatula* root. *Plant Cell* **27**: 3410–3424.

Vincent JM. 1970. *A manual for the practical study of the root-nodule bacteria (IBP Handbk 15).* Oxford and Edinburgh, UK: Blackwell Scientific Publications.

Xu H, Li Y, Zhang K, Li M, Fu S, Tian Y, Qin T, Li X, Zhong Y, Liao H. 2021. *miR169c-NFYA-C-ENOD40* modulates nitrogen inhibitory effects in soybean nodulation. *New Phytologist* **229**: 3377–3392.

Yamaguchi N, Winter CM, Wu MF, Kanno Y, Yamaguchi A, Seo M, Wagner D. 2014. Gibberellin acts positively then negatively to control onset of flower formation in *Arabidopsis*. *Science* **344**: 638–641.

Yamaguchi S. 2008. Gibberellin metabolism and its regulation. *Annual Review of Plant Biology* **59**: 225–251.

Yoro E, Suzaki T, Toyokura K, Miyazawa H, Fukaki H, Kawaguchi M. 2014. A positive regulator of nodule organogenesis, NODULE INCEPTION, acts as a negative regulator of rhizobial infection in *Lotus japonicus*. *Plant Physiology* **165**: 747–758.

Supporting Information

Additional Supporting Information may be found online in the Supporting Information section at the end of the article.

Fig. S1 *GmGA20ox1a* transcripts.

Fig. S2 Genome editing in soybean using CRISPR/Cas9 system.

Fig. S3 Bioactive GA gradients in an emerged lateral root (a) and GPS1-not responsive (NR) vector transformed control nodules (b and c). Bar, 100 μm.

Fig. S4 Nodulation phenotyping upon exogenous GA_3 or PAC treatment.

Fig. S5 *pBjGroESL4::DsRed2*-expressing *B. diazoefficiens*.

Fig. S6 Early nodulation gene expression is upregulated by GA_3 treatment and rhizobia inoculation.

Fig. S7 GA20 oxidase phylogenetic tree.

Fig. S8 GA3 oxidase phylogenetic tree.

Fig. S9 GA2 oxidase phylogenetic tree.

Fig. S10 *GmGA20ox* CDS sequence alignment.

Table S1 List of Gene IDs.

Table S2 List of primers used in this article.

Table S3 List of selection antibiotics used in this article.

Table S4 Expression of GmGA oxidase genes (RNA-seq data) in roots inoculated with wild-type and *nodC*$^{-}$ *Bradyrhizobium diazoefficiens* at 48 hpi.

Please note: Wiley Blackwell are not responsible for the content or functionality of any Supporting Information supplied by the authors. Any queries (other than missing material) should be directed to the *New Phytologist* Central Office.